

- [23] X. B. Wu, P. Chen, J. Lin, K. L. Tan, *Int. J. Hydrogen Energy* **2000**, *25*, 261.
 [24] Z. H. Chen, Y. M. Xie, J. Li, *Chem. J. Chin. Univ.* **1997**, *18*, 1534.
 [25] L. Duclaux, *Carbon* **2002**, *40*, 1751.
 [26] F. H. Moser, A. L. Thomas, *The Phthalocyanines*, 2nd ed., CRC, Boca Raton, FL **1983**.
 [27] I. W. Chiang, R. E. Smalley, R. H. Hauge, *J. Phys. Chem. B* **2001**, *105*, 1157.

Charge Density and Film Morphology Dependence of Charge Mobility in Polymer Field-Effect Transistors**

By Sagi Shaked, Shay Tal, Yohai Roichman, Alexey Razin, Steven Xiao, Yoav Eichen, and Nir Tessler*

The electronic transport in organic semiconducting polymers have been studied extensively in the past decades.^[1–9] Among the physical pictures suggested, the most widely accepted one is that of “hopping-transport” in a disordered system which has a Gaussian density of states (DOS), developed by Bässler and co-workers.^[1,3] However, despite the success of this physical model in describing phenomena related to organic light-emitting diodes (LEDs) it is rarely used to describe charge transport in organic field effect transistors (FETs). This may be partially due to the lack of theoretical predictions as to the effect of the charge density on the mobility and diffusivity. Recently, the disorder picture has been extended to the high-carrier-density regime.^[10] It has been shown, within the disorder model, that the density of the charge carriers affects both the ratio between the mobility and diffusivity (Einstein relation),^[10] and the mobility value.^[11,12] One of the predictions made by the model developed by Roichman and Tessler^[10] is that the important parameter is the charge density relative to the electronic density of states. In this paper we present experimental investigation of the effect of the charge density as well as the film morphology on the charge carrier mobility in poly(2-methoxy-5-(2'-ethylhexyloxy)-1,4-phenylenevinylene) (MEH-PPV)^[13] polymer FETs and make a qualitative comparison with theoretical predictions.

The advantage of investigating MEH-PPV is that it has been extensively studied and is widely available. Within the context of exciton and interchain-exciton generation it has been shown that the use of poor solvents with MEH-PPV

tends to affect the film morphology,^[14–16] as well as interchain interactions. A possible implication for the charge transport was given as mobility enhancement in an LED device configuration^[15] or in a FET configuration.^[17] In the context of charge transport it has also been suggested by Rakhmanova and Conwell^[2] that in the polymer film there are regions that are better ordered and hence exhibit a narrower (Gaussian) DOS. This morphological effect was shown to affect the field dependence of the mobility. In this work we chose to control the solubility parameter by varying the polymer molecular weight rather than the solvent. In this manner we arrive at a systematic set of film morphologies and for each case we study the charge concentration effect on the charge mobility.

Figure 1 shows the photoluminescence (PL) spectra of three weight-average molecular weights of MEH-PPV ($M_w = 100 \text{ kg mol}^{-1}$ (100 k), 1000 kg mol^{-1} (1 M), 2800 kg mol^{-1}

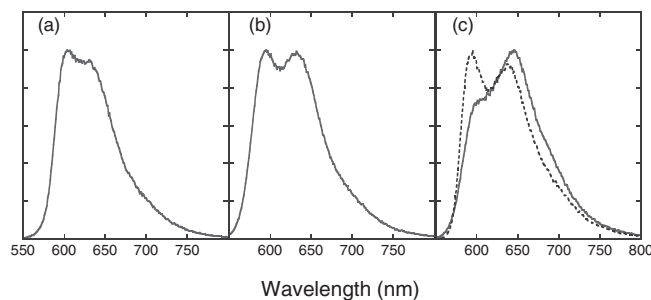


Fig. 1. PL spectra of MEH-PPV films spin cast from toluene. a) $M_w = 100\,000$, b) $M_w = 1\,000\,000$, c) $M_w = 2\,800\,000$. Note the red-shift in the PL spectra as a function of molecular weight indicating enhanced aggregation (density). The dashed line in (c) is for a film cast from THF.

(2.8 M)) spin-cast from toluene. The figure shows a pronounced red-shift as the molecular weight increases. In past solubility studies of MEH-PPV^[14,15] this has been assigned to the formation of aggregates. The PL spectrum of the high- M_w polymer in tetrahydrofuran (THF) is also shown, and this confirms that the spectral shift is indeed solvent- (solubility-) related. To further check if the spectral shifts are also associated with morphological changes, we analyzed the three polymers (spin-cast from toluene) using a scanning atomic force microscope (AFM)^[18] operating in the phase mode. Figure 2 shows the data collected for MEH-PPV films prepared in the same manner as those studied in Figure 1. The morphological differences between the different films are expressed in the different film AFM tip interactions. The film of the low- M_w polymer (100 k) appears as a rather homogeneous, non-sticky, solid film that induces only minor phase shifts to the tip resonant vibration. Only very few isolated spots appear to have stronger film–AFM tip interactions that cause a larger phase shift. In contrast, the film of the high- M_w polymer (2.8 M) appears as a viscoelastic sticky medium with isolated solid islands. The film of the intermediate- M_w polymer (1 M) seems to be composed of a mixture of the two, showing a mix of solid and viscoelastic domains. A strong correlation is found between the phase shift and the height of the different domains. Similar observations were reported using the contact

[*] Prof. N. Tessler, S. Shaked, Y. Roichman, A. Razin
 Electrical Engineering Dept.
 Microelectronic Center, Technion
 Haifa 32000 (Israel)
 E-mail: nir@ee.technion.ac.il
 S. Tal, Prof. Y. Eichen
 Chemistry Dept., Technion
 Haifa 32000 (Israel)

Dr. S. Xiao
 American Dye Source Inc.
 555 Morgan Blvd., Baie D'Urfe, Quebec, H9X 3T6 (Canada)

[**] This research (No. 56/00-11.6) was supported by the Israel Science Foundation.

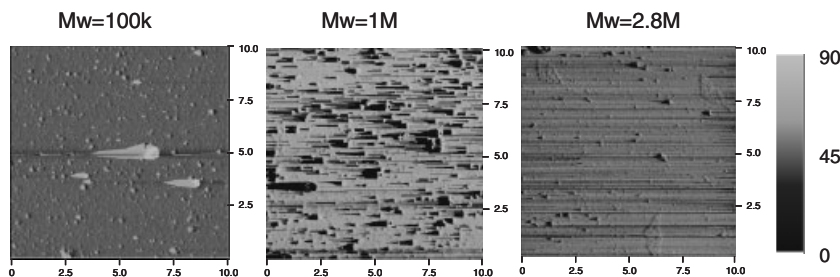


Fig. 2. A $10\ \mu\text{m} \times 10\ \mu\text{m}$ scan of the three MEH-PPV polymers (spin-cast from toluene). The data presented was collected in the phase mode.

topography method for MEH-PPV cast from different solvents.^[15] We emphasize that although none of the films exhibit any pure phase, the relative magnitude of the phases is different enough to allow one to differentiate the three films.

The above polymers were used to prepare FETs in the bottom contact configuration.^[19] The channel length was varied between 2 and $32\ \mu\text{m}$ and the width was fixed at $6000\ \mu\text{m}$ ($C_{\text{ox}} \approx 43\ \text{nF cm}^{-1}$). Extra care was given to remove any residual effects resulting from the device structure^[19,20] that may interfere with the device material analysis. Figure 3 shows the drain/source current as a function of gate bias ($V_{\text{GS}} < 0$) for a given drain/source bias of $-2\ \text{V}$. First we examine the thresh-

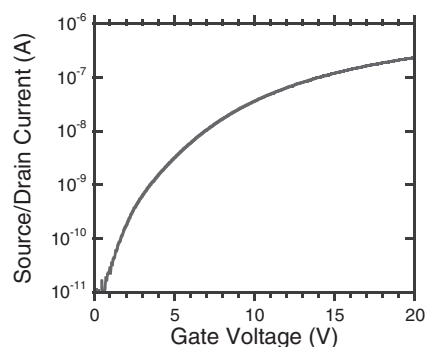


Fig. 3. Source/drain current measured as a function of negative gate voltage. The drain source voltage was $-2\ \text{V}$. At about $0.5\ \text{V}$ the drain/source current exceeds the parasitic charging currents. The channel length is $L = 2\ \mu\text{m}$ and its width is $W = 6000\ \mu\text{m}$ and the polymer used was MEH-PPV ($M_w = 2.8\ \text{M}$).

old voltage (V_{T}) which is an indication of defects occurring at the polymer–oxide interface due to either the polymer or the oxide. As the polymer is undoped, a large contribution to the threshold voltage may arise only from charged defects in the oxide or the polymer.^[21] We find that the current onset is effectively $V_{\text{T}} \approx 0$ indicating that both the oxide and the polymer are relatively free of charged defects. Further indication for the good material and device properties is given by the high on/off ratio which is close to 10^5 (a high number for MEH-PPV). All devices used in this work had a similar threshold voltage. As a general rule, we found that the reliability of the material parameters degrades in devices that exhibit threshold voltages above $4\ \text{V}$ and that such high threshold values are generally due to imperfect device processing procedures.

As in this paper we are concerned with density-dependent mobility the issue of threshold voltage requires some discus-

sion. If the mobility is constant then one can extract the threshold voltage from the known expression:

$$I_{\text{DS}} = K\mu \left([V_{\text{GS}} - V_{\text{T}}] V_{\text{DS}} - \frac{V_{\text{DS}}^2}{2} \right) \quad (1)$$

by fitting the formula for the drain/source current as a function of either the gate/source or the drain/source voltage with the other voltage being fixed. If the mobility is charge-density dependent then it is obviously gate/source voltage dependent but only slightly dependent on the drain/source voltage. In this case, using the $I_{\text{DS}}(V_{\text{GS}})$ curve to extract the threshold voltage may be problematic. Figure 4 shows the common method for extracting V_{T} from $I_{\text{DS}}(V_{\text{GS}})$ curve. A linear line is fitted to the curve for $|V_{\text{GS}}| \gg |V_{\text{DS}}|$ and extrapolated to $I_{\text{DS}} = 0$ to yield the threshold voltage (in this case we arrive at $V_{\text{T}} = 10\ \text{V}$). However, the inset to Figure 4 shows the $I_{\text{DS}}(V_{\text{DS}})$ curves for $V_{\text{GS}} = -7\ \text{V}$ and $V_{\text{GS}} = -10\ \text{V}$ where the

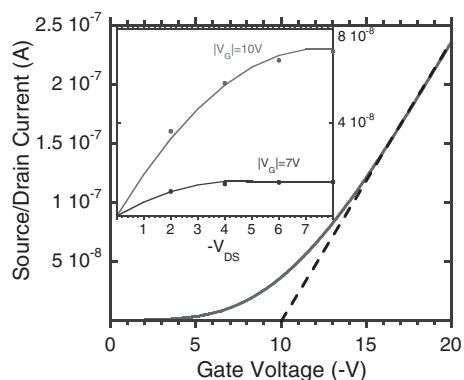


Fig. 4. Source/drain current measured as a function of negative gate voltage (same data as in Fig. 3). The dashed line is a linear fit to the curve in the 16 to $20\ \text{V}$ range. The inset shows the source/drain current measured as a function of drain/source voltage for two different gate voltages, $-7\ \text{V}$ and $-10\ \text{V}$.

shape of both curves suggests that the threshold voltage is well below $10\ \text{V}$. Assuming that the mobility does not depend on the drain/source voltage (not strictly correct), we fit each curve separately requiring a common threshold voltage. We deduce $V_{\text{T}} = 2.5\ \text{V}$ and $\mu \approx 10^{-5}$ and $2 \cdot 10^{-5}\ \text{cm}^2\ \text{V}^{-1}\ \text{s}^{-1}$ for $V_{\text{GS}} = 7\ \text{V}$ and $10\ \text{V}$, respectively. From the above we can safely deduce that the mobility is charge-density-dependent and that the threshold voltage is between $0\ \text{V}$ to $2.5\ \text{V}$.

Based on the above, results as in Figure 3 can be used to determine the field effect mobility^[22] from Equation 1 using a

threshold value in the range 0 to 2.5 V. Using Equation 1 with $V_T = 0$ we calculated the field-effect mobility as a function of gate bias. As the mobility is charge-density (gate-bias) dependent^[23–25] we can assume a constant mobility value across the channel only for $V_{GS} \gg V_{DS}$ or when Equation 1 reduces to

$$I_{DS} = K\mu([V_{GS} - V_T]V_{DS}) \quad (2)$$

Based on the above, we consider the low voltage (very low mobility) values to be of less significance and hence we usually plot the results on a linear scale.

Figure 5 shows the mobility value as extracted for the different M_w PPVs spin-coated from toluene to ~100 nm thick films. We note a clear trend in the mobility value: as the M_w is

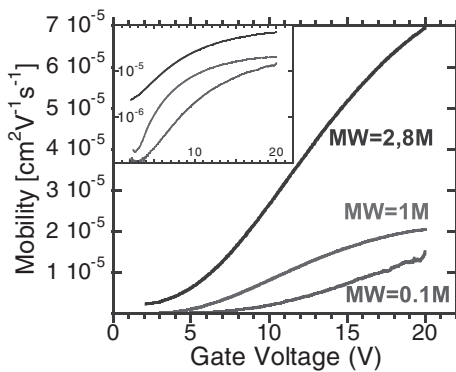


Fig. 5. Mobility as a function of gate voltage for MEH-PPV of three M_w s. The difference between them is almost a constant factor of 3.3.

increased from 100 k to 2.8 M the mobility goes up by about an order of magnitude. We also find that all three polymers exhibit a gate voltage (charge density) dependence of the mobility. A common, secondary, feature is that the slope has a maximum value at an intermediate gate bias value (S shape). For the sake of completeness we show in the inset to Figure 5 the same data but on a semi-log scale. We note that for about an order of magnitude in $(V_{GS} - V_T)$, we find a change in the mobility values of up to two orders of magnitude.

Previous reports of gate-voltage-dependent mobility^[24,25] attributed this effect to the presence of traps. In this paper we suggest that the physical mechanisms (a material property) governing the gate bias dependence of the mobility can be understood using the same physical picture often used for trap-free polymer LEDs,^[2,3,26] namely, a disordered material having a Gaussian DOS of a given width σ . We consider a hypothetical film where one can arbitrarily and independently change the charge density in the film and the electric field applied to it. The calculation is the same as presented previously^[11] and will be extensively discussed in the near future. The model is used here only in the low-electric-field limit which is applicable to the operating conditions of the FETs used in this paper ($|E_{DS}| = 2V/2 \mu\text{m} = 10^4 \text{ Vcm}^{-1}$). In short, to calculate the mobility we assume that the charge carriers hop between localized states according to “Miller–Abrahams” rate,^[27] and that the charge carrier population is in quasi-equilibrium.

The potential drop between the sites is calculated as the distance between sites times the electric field ($R_{ij} \cdot E$). The occupation probability of the state at energy ϵ_i at a certain site is determined by Fermi–Dirac distribution $f(\epsilon_i)$. The total current is the integration on the contribution from the hops from state i to state j , according to the following expression:

$$\bar{J}_{ij} = v_{ij}(R_{ij}, \epsilon_i, \epsilon_j)g(\epsilon_i)f(\epsilon_i, \epsilon_F)g(\epsilon_j)[1 - f(\epsilon_j, \epsilon_F)]R_{ij} \cdot \hat{E} \quad (3)$$

where v_{ij} is the Miller–Abrahams hopping rate from site i to site j , and $g(\epsilon)$ is the DOS at energy ϵ , $g(\epsilon_i)f(\epsilon_i, \epsilon_F)$ is the probability that site i is occupied, and $g(\epsilon_j)[1 - f(\epsilon_j, \epsilon_F)]$ is the probability that site j is empty. From the total current one can then deduce the mobility as $\mu = J/qpE$ with p being the charge density.

Since there is a range of parameters one can use for the width σ , and a combination of widths, we limit ourselves, here, to the methodology and parameters employed by Rakhmanova and Conwell,^[2] who used Monte Carlo simulations to shed light on the field dependence of the mobility in MEH-PPV films. Namely, the MEH-PPV films are assumed to be composed of two phases characterized by a different DOS widths of $8kT$ and $12kT$. This notion is also supported by the AFM images shown in Figure 2. Figure 6 presents the calculation using the same material parameters as Rakhmanova and Conwell.^[2] Firstly, we calculate the density dependence of the

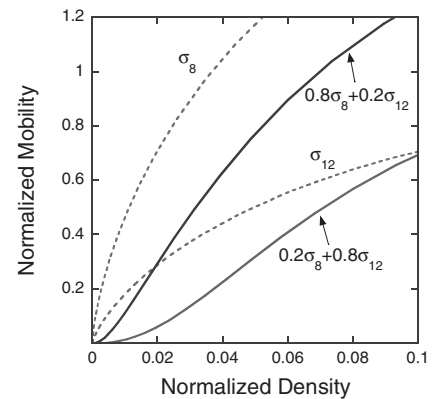


Fig. 6. Calculation of the density dependent mobility for several density of states functions.

mobility for homogeneous samples of $\sigma = 8kT$ (top dashed line) and $\sigma = 12kT$ (lower dashed line). We note that within the disorder-model framework developed by Bässler and co-workers^[3] it is possible to account for strong density dependence of the mobility. It is also clear that the shape of the curves describing the homogeneous samples is somewhat different to the experimental one. Hence, following Rakhmanova and Conwell^[2] we calculated the mobility of an inhomogeneous sample. The solid lines are for inhomogeneous samples having 80 % of $\sigma = 8kT$ and 20 % of $\sigma = 12kT$ (upper line), or 20 % of $\sigma = 8kT$ and 80 % of $\sigma = 12kT$ (lower line). The comparison of Figures 5 and 6 suggests that the inhomogeneous nature of the MEH-PPV film must be accounted for also in

the modeling of the density dependence of the mobility in these films, since only then is an S shape of the mobility curve predicted by the theory. This point is strengthened by the comparison of the calculation presented on semi-log scale (Fig. 7) to the experimental ones (inset to Fig. 5). The effect of mixing two different Gaussian widths is also essential to make the mobility vary by up to two orders of magnitude across an order of magnitude change in the charge density.

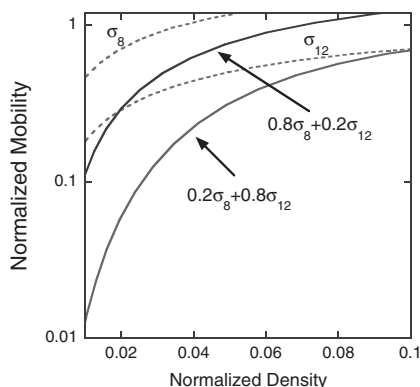


Fig. 7. The same calculation as in Figure 6 but on a semi-log scale.

To summarize, we have presented a systematic study of the effect of the M_w of MEH-PPV on the transport properties in FETs. We found that a critical effect is that of the morphology and film inhomogeneity as a function of the molecular weight. The dependence of the film morphology on the molecular weight is found to be largely due to the effect of the reduced solubility. We found that the presence of inhomogeneity not only affects the field dependence of the mobility,^[2] but also the charge density dependence of it. By employing a recently developed extension^[11] to the disorder model, we could qualitatively reproduce the experimental data, thus suggesting that the disorder model can be used to describe not only LEDs, but also FETs. Namely, the density dependence does not require extrinsic traps to be introduced into the physical picture. Finally, in this paper we do not try to directly reproduce the experimental results but mainly reproduce its functional form. The data presented in Figure 2 clearly shows that assuming only two phases in the films is just an approximation (though much better than the single-phase picture). We believe that as more material information becomes available (such as the DOS), exact modeling and data fitting may become a valid task. Such fitting procedure would be further complicated by the change in the Einstein coefficient at high densities (by a factor of η) as predicted by Roichman and Tessler.^[10] The increase in the Einstein relation enhances the channel width

$$\left(L_D = \sqrt{\frac{kT\epsilon\epsilon_0}{q^2} \cdot \frac{\eta}{p}} = \frac{1}{pq} \sqrt{kT\epsilon\epsilon_0 \cdot \eta p} \right) \quad (4)$$

and hence reduces the charge density at the channel:

$$\left(p = \frac{1}{\eta} [(V_{GS} - V_T)C_{ox}]^2 \frac{1}{q \frac{kT}{q} \epsilon\epsilon_0} \right) \quad (5)$$

Experimental

P++ silicon substrates were used as the gate contact. A high-quality silicon oxide layer (~100 nm) was thermally grown to form the gate dielectric. Ti/Gold was thermally evaporated and patterned to form interdigitated source and drain contacts. Care was taken not to expose the dielectric layer to any contamination during the processing procedure. The polymers were spin-coated from toluene in an inert glove box. All films were annealed under dry vacuum at 90 °C within the glove box.

MEH-PPV with molecular weights ranging from 100 000 to 2 800 000 were synthesized at American Dyes Source Inc. in gram quantities and were used as prepared. Molecular weight was determined via gel permeation chromatography on a Waters Breeze system, calibrated using polystyrene standards.

Topography and phase AFM images were recorded on a DI3100 (Veeco) AFM. Scans were performed using RTESP7 silicon tips (Veeco) in the tapping mode at a scan rate of 2 Hz (tip velocity = 39.4 $\mu\text{m s}^{-1}$).

Received: November 19, 2002
Final version: February 24, 2003

- [1] H. Bässler, *Phys. Status Solidi B* **1993**, *175*, 15.
- [2] S. V. Rakhmanova, E. M. Conwell, *Appl. Phys. Lett.* **2000**, *76*, 3822.
- [3] M. Van der Auweraer, F. C. Deschryver, P. M. Borsenberger, H. Bässler, *Adv. Mater.* **1994**, *6*, 199.
- [4] C. O. Yoon, M. Reghu, D. Moses, A. J. Heeger, Y. Cao, T. A. Chen, X. Wu, R. D. Rieke, *Synth. Met.* **1995**, *75*, 229.
- [5] A. J. Campbell, M. S. Weaver, D. G. Lidzey, D. D. C. Bradley, *J. Appl. Phys.* **1998**, *84*, 6737.
- [6] T. Li, J. W. Balk, P. P. Ruden, I. H. Campbell, D. L. Smith, *J. Appl. Phys.* **2002**, *91*, 4312.
- [7] Y. L. Shen, M. W. Klein, D. B. Jacobs, J. C. Scott, G. G. Malliaras, *Phys. Rev. Lett.* **2001**, *86*, 3867.
- [8] D. J. Pinner, R. H. Friend, N. Tessler, *J. Appl. Phys.* **1999**, *86*, 5116.
- [9] H. Sirringhaus, P. J. Brown, R. H. Friend, M. M. Nielsen, K. Bechgaard, B. M. W. Langeveldvoss, A. J. H. Spiering, R. A. J. Janssen, E. W. Meijer, P. Herwig, D. M. de Leeuw, *Nature* **1999**, *401*, 685.
- [10] Y. Roichman, N. Tessler, *Appl. Phys. Lett.* **2002**, *80*, 1948.
- [11] Y. Roichman, N. Tessler, *Synth. Met.* **2003**, *135–136*, 443.
- [12] V. I. Arkhipov, P. Heremans, E. V. Emelianova, G. J. Adriaenssens, H. Bässler, *J. Phys.: Condens. Matter* **2002**, *14*, 9899.
- [13] D. Braun, A. J. Heeger, *Appl. Phys. Lett.* **1991**, *58*, 1982.
- [14] C. J. Collison, L. J. Rothberg, V. Treemanekarn, Y. Li, *Macromolecules* **2001**, *34*, 2346.
- [15] T. Q. Nguyen, I. B. Martini, J. Liu, B. J. Schwartz, *J. Phys. Chem. B* **2000**, *104*, 237.
- [16] G. Rumbles, I. D. W. Samuel, L. Magnani, K. A. Murray, A. J. De Mello, B. Crystall, S. C. Moratti, B. M. Stone, A. B. Holmes, R. H. Friend, *Synth. Met.* **1996**, *76*, 47.
- [17] W. Geens, S. E. Shaheen, B. Wessling, C. J. Brabec, J. Poortmans, N. S. Sariciftci, *Org. Electron.* **2002**, *3*, 105.
- [18] A. C. Arias, J. D. Mackenzie, R. Stevenson, J. J. M. Halls, M. Inbasekaran, E. P. Woo, D. Richards, R. H. Friend, *Macromolecules* **2001**, *34*, 6005.
- [19] Y. Roichman, N. Tessler, *Appl. Phys. Lett.* **2002**, *80*, 151.
- [20] N. Tessler, Y. Roichman, *Appl. Phys. Lett.* **2001**, *79*, 2987.
- [21] S. M. Sze, *Physics of Semiconductor Devices*, Wiley, New York **1981**.
- [22] A. R. Brown, C. P. Jarrett, D. M. de Leeuw, M. Matters, *Synth. Met.* **1997**, *88*, 37.
- [23] D. Moses, personal communication.
- [24] C. D. Dimitrakopoulos, S. Purushothaman, J. Kymissis, A. Callegari, J. M. Shaw, *Science* **1999**, *283*, 822.
- [25] G. Horowitz, M. E. Hajlaoui, R. Hajlaoui, *J. Appl. Phys.* **2000**, *87*, 4456.
- [26] a) Y. Preezant, N. Tessler, *J. Appl. Phys.* **2003**, *93*, 2059. b) Y. Preezant, Y. Roichman, N. Tessler, *J. Phys.: Condens. Matter* **2002**, *14*, 9913.
- [27] A. Miller, E. Abrahams, *Phys. Rev.* **1960**, *120*, 745.